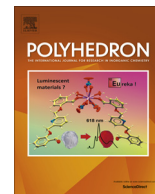




Contents lists available at ScienceDirect

Polyhedron

journal homepage: www.elsevier.com/locate/poly

Ruthenium-8-quinolinethiolate-phenylterpyridine versus ruthenium-bipyridine-phenyl-terpyridine complexes as homogeneous water and high temperature stable hydrogenation catalysts for biomass-derived substrates

Ryan J. Sullivan^a, Jin Kim^b, Caroline Hoyt^b, Louis A. (Pete) Silks III^b, Marcel Schlaf^{a,*}

^a Department of Chemistry, University of Guelph, The Guelph-Waterloo Centre for Graduate Work in Chemistry (GWC)², 50 Stone Road East, Guelph, Ontario N1G 2W1, Canada

^b Los Alamos National Laboratory, Biosciences Division, Group B11, MS E529, P.O. Box 1663, Los Alamos, NM 87545, United States

ARTICLE INFO

Article history:

Received 14 August 2015

Accepted 28 October 2015

Available online xxx

Keywords:

Homogeneous catalysis

Hydrodeoxygenation

Biomass

Ruthenium complexes

Aqueous media

ABSTRACT

[(4'-Ph-terpy)(bipy)Ru(L)](OTf)_n and [(4'-Ph-terpy)(quS)Ru(L)](OTf)_n (*n* = 0 or 1 depending on the charge of L, L = labile ligand, e.g., H₂O, CH₃CN or OTf, bipy = 2,2'-bipyridine, quS = quinoline-8-thiolate) have been evaluated as catalysts for the hydrogenation of the biomass-derivable C6-substrates 2,5-dimethylfuran (obtainable from 5-hydroxymethylfurfural) and 2,5-hexanedione (the hydrolysis product of 2,5-dimethylfuran). Operating in aqueous acidic medium at *T* = 175–225 °C the bipy complex is only marginally active, while the quinoline-8-thiolate complex realizes yields of hydrogenated products up to 97% starting from 2,5-hexanedione and up to 66% starting from 2,5-dimethylfuran. The catalyst can also convert the 5-HMF derived acetone 4-(5-methyl-2-furanyl)-3-buten-2-one into 2,5,8-nonatriol, a potentially valuable cross-linker for polymer formulations. On the basis of DFT calculations, the higher activity of the quinoline-8-thiolate complex is proposed to be rooted in a metal–ligand bifunctional mechanism for the heterolytic activation and transfer of dihydrogen to the carbonyl substrate with the hydride-thiol complex [(4'-Ph-terpy)(quSH)Ru(H)]⁺ as the active catalyst.

© 2015 Published by Elsevier Ltd.

1. Introduction

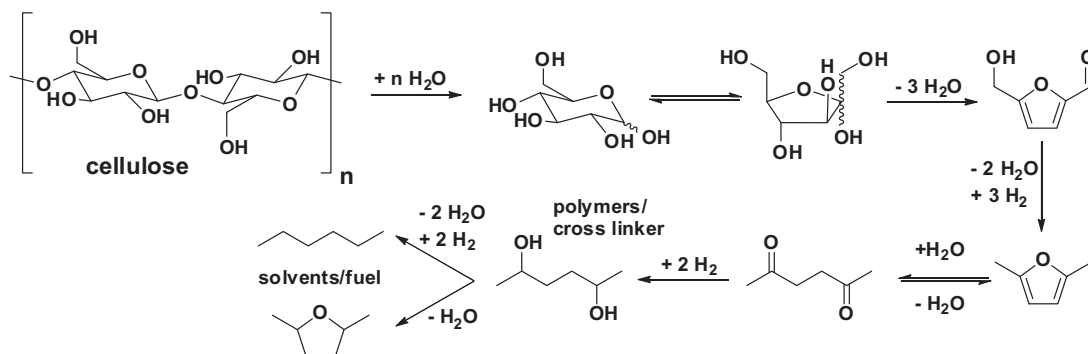
We recently demonstrated the use of the complexes [(4'-Ph-terpy)Ru(H₂O)₃](OTf)₂ (**1**) and [(4'-Ph-terpy)Ir(OTf)₃] (**2**) (4'-Ph-terpy = 4'-phenyl-2,2':6',2''-terpyridine, OTf = trifluoromethanesulfonate) as homogeneous catalysts for the hydrodeoxygenation (HDO) of 2,5-hexanedione (2,5-HD) and 2,5-dimethyl-furan (2,5-DMF) to 2,5-hexane-diol (2,5-HDO) and 2,5-dimethyltetrahydrofuran (2,5-DMTHF) in aqueous acidic medium in up to 69% and 80% yield, respectively. Hexane can also be generated by catalyst **1** in up to 10% yield as the total HDO product [1]. These substrates form part of the value chain shown in Scheme 1 leading from glucose (obtainable from starch, sugarcane/beets or, in principle, cellulose) via the key intermediates 5-hydroxymethylfurfural (HMF) and 2,5-DMF to ultimately hexane [2], with the ultimate goal of our research approach being the development of a robust, recyclable and promiscuous homogeneous acid/metal-based binary catalyst system that through an iterative dehydration/hydrogenation

reaction cascade can directly convert sugars or sugar alcohols to value-added HDO products in a single reactor with water as the only side-product. By definition, this goal requires the catalyst used to be stable to both acid and water, as well as the high temperatures needed – empirically *T* > 150 °C – to trigger the acid catalyzed dehydration reactions of the (poly-) alcohol substrates [3,4].

As a result of our study we found that while complexes **1** and **2** are active and stable in aqueous-acidic medium at temperatures up to 175 °C, they decompose to the inactive bis-tridentate [M(4'-Ph-terpy)₂]ⁿ⁺, M = Ru/*n* = 2 or M = Ir/*n* = 3 complexes at *T* > 175 °C, which were recovered from the reaction mixtures and analyzed by MS and single-crystal X-ray analysis. Furthermore, re-addition of fresh substrate to recovered clear-red reaction solutions of **1** showed only marginal catalytic activity, which – in addition to the formation of the bis-tridentate complex – was attributed to catalyst inhibition by irreversible coordination of organic (by-) products in the reaction, possibly dimers formed by aldol condensation or Diels–Alder adducts acting as chelating ligands. As **1** is postulated to operate as an ionic hydrogenation catalyst with water acting as the base deprotonating a transient η²-H₂ ligand it intrinsically generates one equivalent of acid, giving H₃O⁺ as

* Corresponding author. Tel.: +1 519 824 4120x53002.

E-mail address: mschlaf@uoguelph.ca (M. Schlaf).



Scheme 1. Value chain from cellulose to deoxygenated value-added products via the two target substrates 2,5-dimethylfuran and 2,5-hexanedione [1].

the strongest possible solvent-leveled acid in aqueous medium. However, increased concentrations of an acid co-catalyst (HOTf) and/or the use of organic co-solvents also suppressed catalyst activity. The inhibition by additional acid can then be understood by disfavoring this deprotonation step, i.e., higher concentrations of H_3O^+ push the hydrogen activation equilibrium $[\text{M}(\eta^2\text{-H}_2)]^+ + \text{H}_2\text{O} \rightleftharpoons \text{M} - \text{H} + \text{H}_3\text{O}^+$ to the left side, away from the hydride complex as the active reducing agent.

On the basis of the established catalyst decomposition pathway to $[\text{Ru}(4'\text{-Ph-terpy})_2]^{2+}$ and the postulated catalyst inhibition by chelating organic species we hypothesized that blocking two of the three coordination sites in **1** occupied by labile ligands (i.e., H_2O , solvent, substrate, etc.) by adding a second bidentate chelating ligand would prevent the decomposition to the bis-tridentate complexes, while still leaving one coordination site for the heterolytic activation of dihydrogen. An obvious and logical choice for this is the complex $[(4'\text{-Ph-terpy})(\text{bipy})\text{Ru}(\text{L})](\text{OTf})_n$ (**3**) ($n = 1$ or 2 depending on the charge of L, L = labile ligand, e.g., H_2O , CH_3CN or OTf , $\text{bipy} = 2,2'\text{-bipyridine}$), as Creutz et al. have previously established that the analogous hydride complex cation $[(\text{terpy})(\text{bipy})\text{Ru}(\text{H})]^+$ can rapidly transfer the hydride ligand to carbonyl acceptors in aqueous medium [5–7]. A further extension is the incorporation of the quinoline-8-thiolate ligand resulting in the complex $[(4'\text{-Ph-terpy})(\text{quS})\text{Ru}(\text{L})](\text{OTf})_n$ (**4**) ($n = 0$ or 1 depending on the charge of L, L = labile ligand, e.g., H_2O , CH_3CN or OTf , $\text{quS} = \text{quinoline-8-thiolate}$). For this system we anticipated that the coordination of the soft anionic sulfur donor to the soft ruthenium centre would result in strong binding of the quS ligand in a stable 5-membered metallacycle and lead to an increased electron density on the metal. This in turn should result in a higher hydride donor ability of the corresponding hydride complex $[(4'\text{-Ph-terpy})$

$(\text{quS})\text{Ru}(\text{H})$] (**4a**) postulated to form under catalytic conditions (H_2 atmosphere and elevated temperature) and also potentially enable a metal–ligand bifunctional heterolytic activation of the transient $\eta^2\text{-H}_2$ ligand into a hydride and coordinated thiol assuming that a *cis* configuration between the hydride and thiol can be structurally realized. This was previously directly observed at low temperature for the complexes $[\text{M}(\eta^2\text{-H}_2)(\text{CO})(\text{quS})(\text{PPh}_3)_2]^+ \rightleftharpoons [\text{M}(\text{H})(\text{CO})(\text{quSH})(\text{PPh}_3)_2]^+$, $\text{M} = \text{Ru}, \text{Os}$ [8,9].

The structural evolution of the catalyst systems and the proposed metal–ligand bifunctional heterolytic activation of dihydrogen by **4** is summarized in Scheme 2.

Here we present the comparative evaluation of complexes **3** and **4** as catalysts for the conversions of the lower half of Scheme 1, i.e., the conversion of 2,5-dimethylfuran and 2,5-hexanedione to deoxygenated/hydrogenated products in aqueous acidic medium.

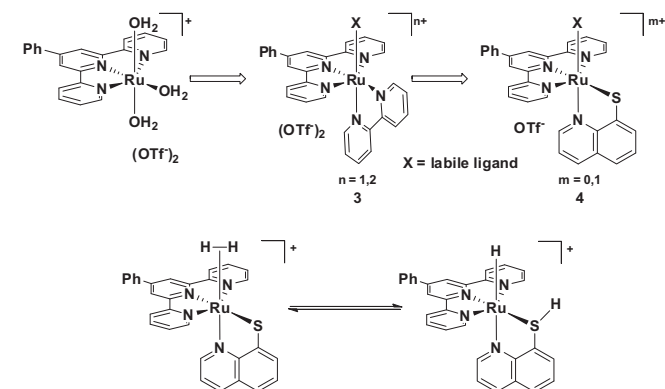
2. Materials and methods

2.1. General

All reagents and solvents were purchased from commercial suppliers and used as received unless otherwise specified. 2,5-HD and 2,5-DMF, 1,4-dioxane and γ -valerolactone were passed through a short plug of neutral Al_2O_3 (Brockmann Activity I) immediately before use to remove any peroxides or stabilizers present and, in the case of 2,5-dimethylfuran, a yellow contaminant of unknown identity (but possibly the 2 + 2 cycloaddition or 4 + 2 Diels–Alder dimer formed under the influence of light). All water used was HPLC grade. NMR spectra were collected on 400 or 600 MHz Bruker Avance spectrometers and calibrated to the residual solvent signals. IR spectra were collected on a Thermo-Fisher Nicolet 4700 FT-IR spectrometer. ESI-MS spectra were collected on Bruker AmaZone SL or Agilent 6540 UHD Accurate Mass Q-TOF spectrometers.

GC analyses were performed on a Varian 3800 with FID detector using a 30 m Stabilwax-da (acid deactivated polyethylene glycol) column. Quantification was carried out using dimethylsulfone as the internal standard (100 mmol L^{-1}) and linear 5 level calibration curves. GC–MS analyses were performed on a Varian Saturn 2000 GC/MS running in CI mode and using the same column and temperature programming used for quantification. Reaction products were identified by comparison to the retention times of authentic samples or by analysis of the mass spectra when authentic samples were unavailable (C_9 HDO products, see SI). Head space gas analyses were carried out on a SRI 8610 micro-GC fitted with a TCD detector against authentic gas samples (1000 ppm of $\text{C}_1\text{--C}_6$ alkanes and alkenes in helium, GRACE Davison Discovery Sciences).

All hydrogenation experiments employed industrial grade H_2 gas (99.995%) and were carried out in an Autoclave Engineers MiniReactor with a 50 mL 316SS reactor vessel and impeller. At a



Scheme 2. Structural evolution of complexes to be tested as catalysts and proposed metal–ligand bifunctional heterolytic activation of dihydrogen by the quinoline-8-thiol complex.

total reaction solution volume of 25 mL the reactor had a gas-phase headspace of ~50 mL (unused reactor body plus enclosed, pressurized magnet-drive assembly). Unless otherwise specified (cf. control experiments) the reactor vessel and impeller were cleaned and polished after each reaction using 3 M abrasive pads or a sand blaster, respectively.

2.2. Chloro(bipy)(4'-Ph-terpy) ruthenium(II) hexafluorophosphate

The procedure reported by Rasmussen et al. for the analogous [RuCl(bipy)(4'-Ph-terpy)](PF₆) was followed substituting phterpy for terpy [10]. RuCl₃(4'-Ph-terpy) (0.501 g, 0.968 mmol), 2,2'-bipyridine (0.167 g, 1.07 mmol) and LiCl (0.204 g, 4.81 mmol) were suspended in 3:1 EtOH:H₂O (100 mL). Triethylamine (1.0 mL, 7.0 mmol) was added and the mixture was purged with Ar for 10 min then refluxed under Ar for 4 h. The deep red-purple solution was cooled to room temperature, filtered then concentrated to half volume and added to 100 mL of saturated, aqueous KPF₆. The resulting red-purple ppt. was collected via filtration, washed with 4 × 10 mL cold 3 M HCl then Et₂O (50 mL). The product was purified by column chromatography (neutral alumina, Brockmann activity I stationary phase, 25 × 300 mm column, 1:1 acetone:toluene eluent). The desired product eluted first as a dark purple band that was collected and evaporated to yield a purple residue. The residue was dissolved in minimal acetonitrile, added to Et₂O (200 mL) and the resulting purple powder was collected by filtration and washed with Et₂O. Yield: 0.462 g; 64%. ¹H NMR: (400 MHz, acetone-d₆, δ): 10.41 (dd, J₁ = 5.6 Hz, J₂ = 0.7 Hz, 1H), 9.10 (s, 2H), 8.93 (d, J = 8.1 Hz, 1H), 8.87 (d, J = 7.9 Hz, 2H), 8.65 (d, J = 8.0 Hz, 1H), 8.44 (dt, J₁ = 7.9 Hz, J₂ = 1.5 Hz, 1H), 8.26 (d, J = 7.1 Hz, 2H), 8.14 (ddd, J₁ = 7.1 Hz, J₂ = 5.6 Hz, J₃ = 1.3 Hz, 1H), 8.03 (dt, J₁ = 7.9 Hz, J₂ = 1.5 Hz, 2H), 7.89 (dd, J₁ = 5.5 Hz, J₂ = 0.7 Hz, 2H), 7.85 (dt, J₁ = 7.6 Hz, J₂ = 0.9 Hz, 1H), 7.71 (t, 2H), 7.70 (d, 1H), 7.64 (t, J = 7.3 Hz, 1H), 7.44 (ddd, J₁ = 7.6 Hz, J₂ = 5.5 Hz, J₃ = 1.3 Hz, 2H), 7.14 (ddd, J₁ = 7.3 Hz, J₂ = 5.8 Hz, J₃ = 1.3 Hz, 1H). ¹³C NMR: (100 MHz, acetone-d₆, δ): 160.67 (C), 160.52 (C), 159.88 (C), 157.94 (C), 154.27 (CH), 153.86 (CH), 153.68 (CH), 147.48 (C), 138.66 (C), 138.45 (CH), 138.18 (CH), 137.12 (CH), 131.49 (CH), 130.99 (CH), 129.17 (CH), 128.88 (CH), 128.42 (CH), 127.91 (CH), 125.40 (CH), 125.10 (CH), 124.92 (CH), 121.73 (CH). ESI-MS: M⁺ peak: 602.07; calc. [C₃₁H₂₃-ClN₅Ru]⁺: 602.07.

2.3. (Bipy)(4'-Ph-terpy)(triflate) ruthenium(II) triflate (3)

The procedure reported by Rasmussen et al. for the analogous [Ru(OTf)(bipy)(4'-Ph-terpy)](OTf) was followed with slight modification [10]. The following was performed with the exclusion of O₂ using standard Schlenk technique. [RuCl(bipy)(4'-Ph-terpy)](PF₆) (0.417 g, 0.558 mmol) was dissolved in 1,2-dichlorobenzene (50 mL) forming a dark purple solution. Triflic acid (0.75 mL, 8.5 mmol) was added resulting in an immediate color change to dark cherry red. The solution was stirred for 4 h at 50 °C then cooled to 0 °C and added to -20 °C Et₂O (200 mL). The resulting solid was filtered and washed with Et₂O. Yield: 0.380 g; 79% dark cherry red powder. The product was contaminated with 9% [Ru(4'-Ph-terpy)₂](OTf)₂ by mass but was used as is for catalysis experiments since the catalytic activity of [Ru(4'-Ph-terpy)₂](OTf)₂ was previously determined to be negligible. NMR and mass spectra were collected in acetonitrile after allowing 2 h at room temperature for replacement of the highly labile triflate by acetonitrile in the sixth coordination site. High purity samples of [Ru(NCMe)(bipy)(4'-Ph-terpy)](OTf)₂ (**3a**) for characterization were produced in low yield (~1%) using column chromatography (alumina neutral, Brockmann activity I, 20 × 300 mm, 2:1 MeCN:toluene eluent). The separation of [Ru(4'-Ph-terpy)₂](OTf)₂ and **3a** was minimal, however collecting only

the tail of the orange-red band that eluted yielded **3a**, after removal of the solvent, as an orange powder in good purity. ¹H NMR: (400 MHz, MeCN-d₃, δ): 9.62 (d, J = 5.4 Hz, 1H), 8.83 (s, 2H), 8.63 (d, J = 8.0 Hz, 1H), 8.58 (d, J = 8.0 Hz, 2H), 8.37 (d, J = 8.1 Hz, 1H), 8.33 (t, J = 7.8 Hz, 1H), 8.13 (d, J = 7.3 Hz, 2H), 8.03 (t, J = 7.8 Hz, 2H), 7.98 (t, J = 6.2 Hz, 1H), 7.81 (t, J = 8.7 Hz, 1H), 7.73 (t, J = 7.1 Hz, 2H), 7.71 (d, J = 4.5 Hz, 2H), 7.66 (t, J = 7.3 Hz, 1H), 7.36 (m, 3H), 7.09 (t, J = 6.2 Hz, 1H). ¹³C NMR: (100 MHz, MeCN-d₃, δ): 159.34 (C), 158.54 (C), 158.51 (C), 156.80 (C), 154.10 (CH), 153.35 (CH), 152.01 (CH), 150.22 (C), 139.40 (CH), 138.52 (CH), 138.27 (CH), 137.47 (C), 131.41 (CH), 130.50 (CH), 128.73 (CH), 128.67 (CH), 128.41 (CH), 127.54 (CH), 126.03 (C), 125.32 (CH), 125.05 (CH), 124.43 (CH), 122.37 (CH). ESI-MS: [M]²⁺ peak: 304.02; calc. [C₃₃H₂₆N₆Ru]²⁺: 304.06.

2.4. Chloro(4'-Ph-terpy)(8-quinolinethiolate) ruthenium(III) chloride

The following was performed with the exclusion of O₂ using standard Schlenk techniques. RuCl₃(4'-Ph-terpy) (0.498 g, 0.964 mmol), 8-quinolinethiol hydrochloride (0.228 g, 1.15 mmol) and sodium bicarbonate (0.194 g, 2.31 mmol) were suspended in methanol (150 mL) and refluxed overnight. The resulting dark red solution was cooled to room temperature and filtered. The solvent was removed *in vacuo* yielding the product as a red powder. Yield 0.599 g; 97%. Small amounts of impurities were present; the product was used without further purification. ESI-MS: M⁺ peak: 605.9; calc. [C₃₀H₂₁ClN₄SRu]⁺: 606.02.

2.5. Acetonitrile(4'-Ph-terpy)(8-quinolinethiolate) ruthenium(II) triflate (4)

[RuCl(quS)(4'-Ph-terpy)]Cl (0.481 g, 0.750 mmol), silver triflate (1.03 g, 4.01 mmol) and zinc powder (0.496 g, 7.69 mmol) were suspended in acetonitrile (150 mL) and refluxed under argon overnight resulting in a deep red solution and off white precipitate. The mixture was cooled to room temperature and filtered. The insoluble materials were discarded. The solvent was removed from the filtrate *in vacuo* resulting in a dark burgundy residue that was purified by column chromatography (neutral alumina, Brockmann activity I stationary phase, 25 × 300 mm column, 1:1 MeCN:toluene eluent). The product eluted first as a dark red band that was collected and evaporated yielding a dark burgundy solid that was stored under argon. Yield: 0.254 g; 44%. ¹H NMR: (400 MHz, MeCN-d₃, δ): 9.66 (dd, J₁ = 5.1 Hz, J₂ = 1.4 Hz, 1H), 8.63 (s, 2H), 8.50 (d, J = 7.9 Hz, 2H), 8.40 (dd, J₁ = 8.4 Hz, J₂ = 1.2 Hz, 1H), 8.06 (d, J = 7 Hz, 2H), 7.94 (t, J = 8.0 Hz, 2H), 7.81 (d, J = 5.4 Hz, 2H), 7.70 (dd, J₁ = 8.3 Hz, J₂ = 5.0 Hz, 1H), 7.65 (t, J = 7.6 Hz, 2H), 7.59 (t, J = 7.2 Hz, 1H), 7.50 (d, J = 7.9 Hz, 1H), 7.42 (d, J = 7.1 Hz, 1H), 7.33 (t, J = 6.3 Hz, 2H), 7.28 (t, J = 7.7 Hz, 1H), 2.01 (s, 3H). ¹³C NMR: (100 MHz, MeCN-d₃, δ): 159.66 (C), 159.15 (C), 154.01 (C), 153.01 (CH), 152.80 (C), 152.32 (CH), 146.93 (C), 137.94 (C), 137.89 (CH), 137.50 (CH), 132.24 (C), 130.80 (CH), 130.73 (CH), 130.28 (CH), 128.41 (CH), 128.15 (CH), 127.93 (CH), 124.39 (CH), 122.91 (CH), 121.07 (C), 120.08 (CH), 120.67 (CH), 4.11 (CH₃). ESI-TOF-MS: [M-MeCN]⁺: 571.0523; calc. [C₃₀H₂₁N₄SRu]⁺: 571.0525.

2.6. Computations

All calculations were performed using the GAUSSIAN 09 software suite [11]. All structures were optimized using the M06-L functional [12,13], with def2-SVP basis set [14] and associated ECP [15] for Ru and 6-31G(d,p) basis set [16–18] for all other atoms. An ultrafine integration grid (99 radial shells with 590 angular points per shell) was used. Solvent effects were incorporated using the polarizable continuum model for water [19–23]. All structures were verified to be local minima or transition states by frequency

calculations showing 0 or 1 imaginary frequencies, respectively. For transition state structures the normal mode vibration corresponding to the imaginary frequency involved motion of the correct atom(s) along the reaction coordinate in all cases. Gibbs free energies reported include zero-point energy corrections and thermal corrections for $T = 473$ K and $p = 55$ atm. Final evaluation of energies was performed using single point energy calculations on the M06-L/def2-SVP,6-31G(d,p) geometries using the M06-L functional, def2-TZVP basis set [14] with associated ECP [15] for Ru and the 6-311G(d,p) basis set [24,25] for all other atoms. Zero-point and thermal energy corrections were taken from the lower level geometry optimizations.

2.7. Purification of 4-(5-methyl-2-furanyl)-3-buten-2-one (C9 substrate)

4-(5-Methyl-2-furanyl)-3-buten-2-one was provided through a collaboration with Los Alamos National Laboratory (LANL) [26]. Prior to use the oily, brown semi-solid (5 g) was sublimed at 40 °C, 60 mTorr to yield a slightly off-white powder that was stored at 4 °C. Yield after sublimation: 4.2 g, mp 30–31 °C (lit. 35–36 °C) [27]. ^1H NMR: (400 MHz, CDCl_3 , δ): 7.20 (d, $J = 15.8$ Hz, 1H), 6.55 (d, $J = 3$ Hz, 1H), 6.53 (d, $J = 16.3$ Hz, 1H), 6.09 (dd, $J_1 = 3.3$ Hz, $J_2 = 0.9$ Hz, 1H), 2.34 (d, $J = 0.8$ Hz, 3H), 2.30 (s, 3H). ^{13}C NMR: (100 MHz, CDCl_3 , δ): 198.04 (C), 156.01 (C), 149.55 (C), 129.64 (CH), 122.67 (CH), 117.73 (CH), 109.30 (CH), 27.99 (CH_3), 14.07 (CH_3).

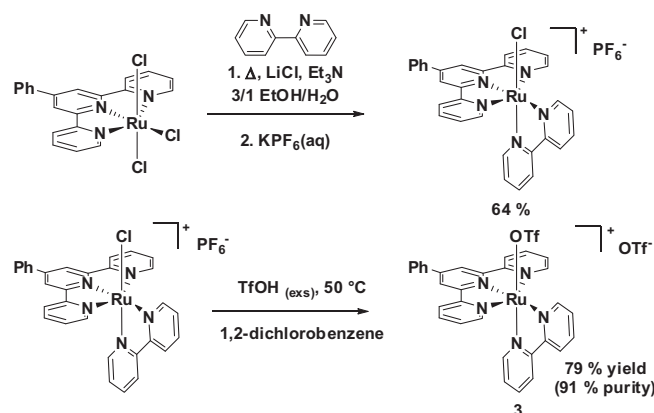
2.8. Example HDO experiment of the C9 substrate

$[\text{Ru}(\text{NCMe})(\text{quS})(4'\text{-Ph-terpy})](\text{OTf})$ (0.0451 g, 0.0593 mmol) and C9 substrate (1.878 g, 12.5 mmol) were charged into an Auto-clave Engineers MiniReactor. Dimethylsulfone (0.236 g, 2.51 mmol, GC internal standard) and water (20 mL) were added and the reactor purged three times with hydrogen. The reactor was pressurized to 55 bar (800 psi) H_2 , sealed and heated to 200 °C. Heating was accomplished in ~30 min. The reaction was stirred at temperature for 16 h then cooled. A sample of the headspace gas was taken for micro-GC analysis before the reactor was vented. The reaction products were analyzed by GC-FID for quantification and GC-MS for identification.

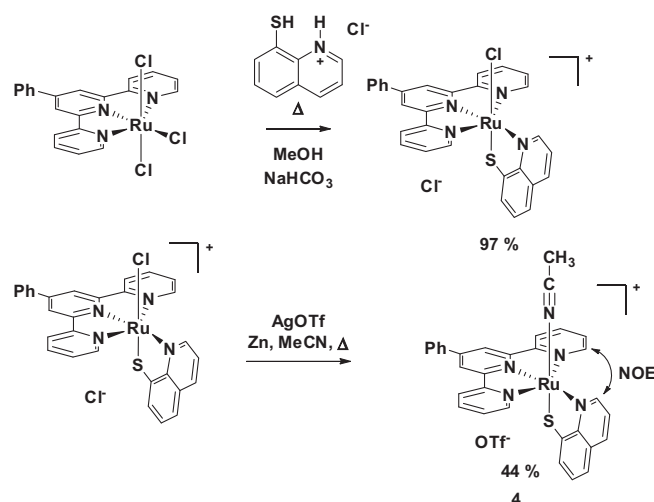
3. Results

3.1. Synthesis and characterization of $[\text{Ru}(\text{OTf})(\text{bipy})(4'\text{-Ph-terpy})](\text{OTf})$ (**3**) and $[(4'\text{-Ph-terpy})(\text{quS})\text{Ru}(\text{NCCH}_3)](\text{OTf})$ (**4**)

$[\text{Ru}(\text{OTf})(\text{bipy})(4'\text{-Ph-terpy})](\text{OTf})$ (**3**) was prepared by modification of the procedure for the analogous $[\text{Ru}(\text{OTf})(\text{bipy})(\text{terpy})](\text{OTf})$ and the synthesis is summarized in Scheme 3 [10]. $\text{RuCl}_3(4'\text{-Ph-terpy})$ was reacted with bipy in aqueous ethanol followed by addition of $\text{KPF}_6(\text{aq})$ to precipitate $[\text{RuCl}(\text{bipy})(4'\text{-Ph-terpy})](\text{PF}_6)$. Anion exchange by treatment of $[\text{RuCl}(\text{bipy})(4'\text{-Ph-terpy})](\text{PF}_6)$ with TfOH in 1,2-dichlorobenzene at 50 °C followed by addition of Et_2O precipitated $[\text{Ru}(\text{OTf})(\text{bipy})(4'\text{-Ph-terpy})](\text{OTf})$ (**3**) in 91% purity, contaminated by 9% of $[\text{Ru}(4'\text{-Ph-terpy})_2](\text{OTf})_2$. Separation of these two compounds proved extremely challenging due to the high (but desired) lability of the triflate ligand in **3**, which resulted in substitution reactions in many solvents. Since the activity of $[\text{Ru}(4'\text{-Ph-terpy})_2](\text{OTf})_2$ had already been shown to be negligible in HDO reactions [1], **3** was therefore used for the catalysis studies without further purification taking into account of the presence of inactive material for the calculation of actual catalyst load. High purity samples of $[\text{Ru}(\text{NCMe})(\text{bipy})(4'\text{-Ph-terpy})](\text{OTf})_2$ (**3a**) for characterization could be prepared by stirring **3** in acetonitrile for 2 h followed by column chromatog-



Scheme 3. Synthesis of $[\text{Ru}(\text{OTf})(\text{bipy})(4'\text{-Ph-terpy})](\text{OTf})$ (**3**).



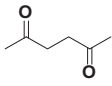
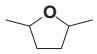
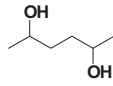
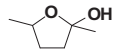
Scheme 4. Synthesis of $[\text{Ru}(\text{NCMe})(\text{QuS})(4'\text{-Ph-terpy})](\text{OTf})$ (**4**).

raphy to separate **3a** from $[\text{Ru}(4'\text{-Ph-terpy})_2](\text{OTf})_2$, but this, however, was not practical for production of quantities sufficient for use in HDO experiments because good resolution could not be achieved between the two products and therefore large sacrifices to yield would have been required to achieve high purity.

The new complex $[\text{Ru}(\text{NCMe})(\text{QuS})(4'\text{-Ph-terpy})](\text{OTf})$ (**4**) was prepared as summarized in Scheme 4. $\text{RuCl}_3(4'\text{-Ph-terpy})$ was reacted with $\text{quSH}\cdot\text{HCl}$ ($\text{quSH}\cdot\text{HCl} = 8\text{-quinolinethiol hydrochloride}$) and NaHCO_3 in MeOH to yield $[\text{RuCl}(\text{quS})(4'\text{-Ph-terpy})]\text{Cl}$. Subsequent reaction with Zn and AgOTf in MeCN followed by column chromatography gave the desired product **4**. Two isomers are theoretically possible. As indicated in Scheme 4, a ^1H NMR-NOE experiment determined that the acetonitrile ligand was located *trans* to the sulfur atom of the quS ligand, i.e., the synthesis gives what appears to be the wrong isomer to facilitate the desired metal–ligand bifunctional heterolytic dihydrogen activation into a hydride and coordinated thiol as proposed in Scheme 2.

Surprisingly, for isolated **4** the IR spectrum displayed only a very weak signal in the nitrile stretching region ($\nu = 2261$ cm^{-1}), which suggested that the acetonitrile ligand might be lost during evaporation of the solvent leading to the complex $\text{Ru}(\text{OTf})(\text{QuS})(\text{phterpy})$ as the actual isolated material. A high-resolution ESI-MS gave a peak matching the molecular weight of **4** minus acetonitrile with a characteristic ruthenium isotope pattern, for which the loss of the labile acetonitrile ligand is however likely an artifact of the method. In contrast, a ^1H NMR experiment in acetone- d_6 showed the signal from the methyl peak of coordinated acetonitrile. The molecular

Table 1
Results of HDO of 2,5-hexanedione by **3** (bipy) and **4** (quS) in water.

Entry ^a	Cat.	T [°C]	2,5-HD ^b [%] 	2,5-DMTHF ^b [%] 	2,5-HDO ^b [%] 	HMA ^b [%] 	MBD ^b [%] <i>Humins</i>	Cat. decomp.
1	3	175	78	1	2	5	14	N
2	3	200	60	6	5	8	21	Y
3	3	225	38	18	3	6	34	Y
4	4	175	0	1	83	2	14	N
5	4	200	0	8	89	0	3	N
6	4	225	3	58	25	6	8	N
7	4	245 ^c	9	50	0	8	34	Y
8 ^d	4	200	0	2	81	9	6	N
9 ^e	4	245 ^c	48	6	0	2	44	n/a
10 ^f	4	245 ^c	55	0	0	0	45	n/a
11 ^g	control	225	81	1	0	0	18	n/a

^a Reaction conditions: 2,5-hexanedione [1000 mmol/L] in water, 5.5 MPa (800 psi) H₂(g), dimethylsulfone (ISTD) [100 mmol/L], catalyst load [1 mmol/L = 0.1% w.r.t. substrate], reaction time = 16 h.

^b By quant. GC-FID; ±1%; 2,5-HD = 2,5-hexanedione; 2,5-DMTHF = 2,5-dimethyltetrahydrofuran; 2,5-HDO = 2,5-hexanediol; HMA = hemiacetal = 2-hydroxy-2,5-dimethyltetrahydrofuran formed by cyclization of the partial hydrogenation product 2-hydroxy-hexan-2-one; MBD = mass balance deficiency: gas phase products and substrate decomposition to polymers and solids (humins) not quantifiable by GC.

^c Maximum sustained internal temperature achievable on the equipment used at time of study.

^d Experiment performed using the burgundy red aqueous phase from entry 5 with fresh substrate added.

^e Control reaction using reactor coating from entry 7.

^f Experiment performed using the burgundy red aqueous phase from entry 7 with fresh substrate added.

^g Control reaction without catalyst added.

weight of the acetonitrile complex was therefore taken for the catalyst load calculations in the catalysis study.

3.2. Catalytic hydrogenations

The results of the catalytic hydrogenation of 2,5-hexanedione (2,5-HD) in water by complexes **3** and **4** are summarized in Table 1.¹ The bipy complex **3** shows only low activity (Entries 1–3) achieving a maximum combined yield of fully hydrogenated products (2,5-DMTHF and 2,5-hexanediol) of only 11% at 200 °C and 21% at 225 °C. This corresponds to a minimum TON of 420 and TOF of only 14 h⁻¹ at 200 °C.² As observed with **1** [1], catalyst decomposition to [Ru(4'-Ph-terpy)₂](OTf)₂ and inactive Ru⁰ was observed at T > 175 °C.

In contrast, the quS complex **4** realizes very high conversions to HDO products (up to 97%, Entry 5, Table 1) and achieves very good mass balances. While the complex is essentially insoluble in water at room temperature, after the reactions the color of the aqueous solution adopt the dark burgundy color of **4**, but small amounts of a burgundy precipitate were also always present. Rinsing the reactor body with MeOH dissolved the burgundy precipitate deposited by reactions at 175 or 200 °C to leave a shiny 316SS surface, i.e., no catalyst decomposition was apparent at this temperature. The solution recovered from the reaction at 200 °C could be recycled with the addition of fresh substrate in a cleaned reactor (Entry 8, Table 1) realizing almost the same amount of 2,5-hexanediol, giving a TON for this catalyst of, at minimum, 3600 and a minimum TOF comparable to that of **1** at 121 h⁻¹.³ At 225 °C a matte,

slight discoloration of the reactor body was observed after rinsing with MeOH following the reaction and a blue metallic Ru⁰ coating was observed after rinsing with MeOH following the reaction at 245 °C (Entries 6 and 7, Table 1). Very similar in appearance to that from decomposition of **1**, the coating formed by decomposition of **4** exhibited negligible HDO activity (Entry 9, Table 1). Instead, a high degree of substrate oligo-/polymerization to non-volatile solids occurred, most likely by aldol condensation reactions. The still clear-red colored solution from the reaction conducted at 245 °C also showed only negligible recyclability, indicating lack of catalyst stability at this temperature (Entry 10, Table 1) by decomposition to inactive [Ru(4'-Ph-terpy)₂](OTf)₂.

The results of applying complex **4** to the conversion of the more directly biomass derivable 2,5-DMF are summarized in Table 2. Due to its low activity further studies with **3** were abandoned. The best result with **4** at 0.1 mol% catalyst load was achieved at 200 °C with 50% yield of 2,5-hexanediol, 11% yield of 2,5-DMTHF and the lowest amount of substrate decomposition (Entry 2, Table 2). As previously observed with **1**, addition of even a small amount of acid (0.5 eq of TfOH w.r.t. **4**, Entry 7, Table 2) also resulted in significant deactivation of the catalyst and was not effective at decreasing the extent of substrate decomposition. Use of the weaker acid HC(O)OH, which decomposes at the reaction temperature (Entry 6, Table 2), resulted in less catalyst deactivation, but also gave no improvement towards minimizing substrate decomposition and the yields were lower than with no acid added. Use of a higher catalyst load, 0.5% w.r.t. substrate (Entry 7, Table 2), resulted in up to 78% yield of 2,5-hexanediol and 9% of 2,5-DMTHF.

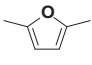
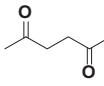
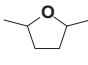
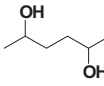
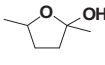
Unfortunately, with the more demanding furan ring containing substrates the recyclability of **4** previously observed for HDO of 2,5-hexanedione was no longer achieved. Since a higher catalyst load was necessary, but the solubility of **4** at room temperature was still very low, the vast majority of catalyst precipitated from solution upon cooling the reactor to room temperature. Thus, in contrast to the reaction with 2,5-HD, the recovered reaction solution is only marginally active upon addition of fresh 2,5-DMF substrate (Entry 5 → 8, Table 2), giving only the hydrolysis ring-opening product 2,5-HD upon recycling. Reuse of the burgundy precipitate deposited on the reactor walls showed some activity

¹ A complete reaction cascade for the HDO of 2,5-HDO and 2,5-DMF is elaborated in Scheme 3 of Ref. [1], which also discusses the most likely pathway in more detail.

² TON estimated based on 2 eq. of H₂ added to each substrate molecule, 0.1% cat load w.r.t. substrate and 21% yield of hydrogenated products at 225 °C. TOF estimated at 200 °C for comparison with other catalysts based on TON = 220 at this temperature and reaction time of 16 h.

³ TON estimated based on 2 eq. of H₂ added to each substrate molecule, 0.1% cat load w.r.t. substrate and 97% and 83% yields of hydrogenated products for the 1st and 2nd reactions respectively. Actual TON could be higher as the catalyst may be usable for additional reactions, and only the amount of catalyst soluble in water at r.t. was used for the second reaction (solids were discarded when the reactor was cleaned). TOF estimated based on TON = 1940 and reaction time of 16 h for the first reaction. The actual TOF could be considerably larger if the majority of hydrogenation occurs in the first couple hours.

Table 2
Results of HDO of 2,5-DMF by **4** in water.

Entry ^a	T [°C]	Cat. load [% w.r.t. substrate]	Acid load [% w.r.t. substrate]	2,5-DMF ^b [%] 	2,5-HD ^b [%] 	2,5-DMTHF ^b [%] 	2,5-HDO ^b [%] 	HMA ^b [%] 	MBD ^b [%] Humins
1 ^c	175	0.1	–	1	1	1	42	1	54
2 ^c	200	0.1	–	0	3	11	50	5	31
3	225	0.1	–	0	15	34	5	9	37
4 ^d	225	control	–	1	82	1	0	0	16
5	200	0.1	0.05/HOTf	0	38	9	7	10	37
6	200	0.1	0.1/HC(O)OH ^e	0	5	5	36	5	49
7	200	0.5	0	0	1	9	78	2	9
8 ^f	200	n/a	0	1	75	2	n/c ^g	5	17
9 ^h	200	n/a	0	1	27	1	15	11	45
10 ⁱ	200	n/a	0	1	41	1	2	5	50

^a Reaction conditions: 2,5-dimethylfuran [1000 mmol/L] in water, 5.5 MPa (800 psi) H₂ (g), dimethylsulfone (ISTD) [100 mmol/L], catalyst load [1 mmol/L = 0.1% w.r.t. substrate], reaction time = 16 h.

^b By quant. GC-FID; ±1%; 2,5-DMF = 2,5-dimethylfuran; 2,5-HD = 2,5-hexanedione; 2,5-DMTHF = 2,5-dimethyltetrahydrofuran; 2,5-HDO = 2,5-hexanediol; HMA = hemiacetal = 2-hydroxy-2,5-dimethyltetrahydrofuran formed by cyclization of the partial hydrogenation products 2-hydroxy-hexan-2-one; MBD = mass balance deficiency: gas phase products and substrate decomposition to polymers and solids (humins) not quantifiable by GC.

^c Solids (substrate polymerization) present after reaction.

^d Control reaction without catalyst.

^e pH before reaction = 3.48; pH after reaction = 5.40; CO₂ peak observed in micro-GC trace of reactor headspace after reaction.

^f Experiment performed by filtering the burgundy red aqueous phase from entry 7 and adding fresh substrate to assess recyclability of the catalyst solution.

^g n/c = not possible to calculate in the recycling experiment: the concentration of 2,5-hexanediol was higher before the reaction than after due to a combination of conversion to 2,5-DMTHF and decomposition.

^h Experiment performed without cleaning any of the burgundy solids generated in entry 7 from the reactor and adding new dimethylsulfone solution and substrate.

ⁱ Experiment performed by rinsing the reactor with MeOH after the reaction of entry 7 but not removing any of the MeOH insoluble discolourations and adding new dimethylsulfone solution and substrate.

(Entry 9, Table 2) but far less than with the addition of fresh catalyst. Further heterogeneous catalysis by Ru⁰ could not be excluded with this experiment. Therefore, the reactor was subsequently rinsed with MeOH to remove the MeOH components of the burgundy precipitate but not any Ru⁰ deposits and the control reaction was repeated. This reaction showed only negligible hydrogenation activity (Entry 10, Table 2), consistent with previous observations for the inactivity of Ru⁰ deposited by **1** and supported the hypothesis that homogeneous catalysis is in fact the origin of the observed hydrogenations. Characterization of the burgundy precipitate deposited in the reactor after reactions showed the presence of both **4** and [Ru(4'-Ph-terpy)₂]²⁺, providing evidence that incorporating quS as a second ligand in conjunction with 4'-Ph-terpy was successful at slowing, but not preventing, bis-chelate formation. This also suggests a possible explanation for the deactivation of **4** by even sub-stoichiometric amounts of acid – either as generated by the activation of H₂ by the complex or by adding more HOTf (Entry 5, Table 2). Once protonated, quS should coordinate less strongly to ruthenium because of the loss of formal negative charge on the ligand and decrease in electron density available for donation from the sulfur atom to the Ru^(II) centre. Therefore, under acidic conditions protonation of the quS ligand may result in loss of free thiol, formation of **1** and then conversion to [Ru(4'-Ph-terpy)₂]²⁺, explaining why activity of **4** was so diminished in the presence of even 0.5 eq w.r.t. **4** of added triflic acid. Formation of [Ru(4'-Ph-terpy)₂]²⁺ also appeared to be acid catalyzed (Scheme 5), since [Ru(4'-Ph-terpy)₂]²⁺ was generated as a by-product at temperatures as low as 50 °C during the preparation of **3** by the reaction of [RuCl(bipy)(4'-Ph-terpy)](PF₆) with excess HOTf in 1,2-dichlorobenzene, explaining why activity associated with **1** formed by loss of quSH was also not observed.

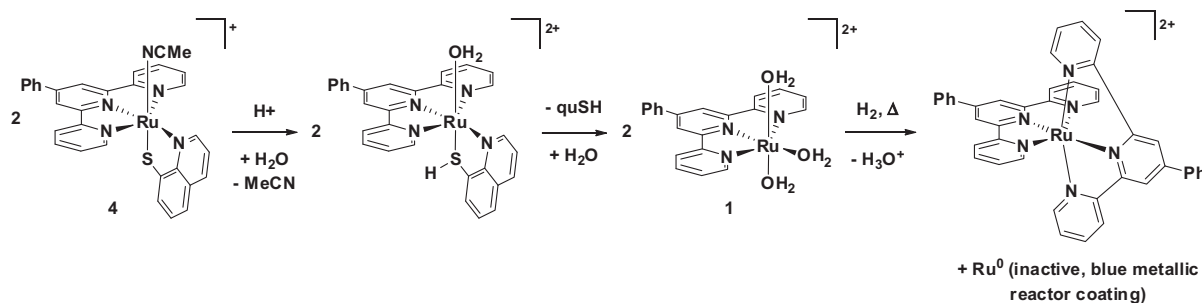
As is evident from the last column (MBD) of Table 2, the 2,5-DMF substrate is under identical reaction conditions (cf. Table 1), much more susceptible to oligo-/polymerization reactions resulting in higher mass balance deficiencies than with 2,5-HD. As previously reported and discussed [1], we attribute this to the low solubility

of 2,5-DMF in water at room temperature. This results in an initially biphasic reaction mixture that has a high concentration of substrate in the organic phase leading to reaction of the substrate with itself, possibly by Diels–Alder reactions, which are not possible with 2,5-HD, or again aldol condensation after ring-opening hydrolysis. This substrate decomposition is also observed to a large extent in the uncatalyzed control reaction (Entry 4, Table 2).

In an attempt to minimize substrate decomposition, the activity of **4** in mixtures of water/sulfolane (1:9), water/1,4-dioxane (1:5), γ -valerolactone (1:9) and pure ethanol (99%), all of which fully dissolve both the catalyst and 2,5-DMF at room temperature, was investigated. While decomposition was greatly reduced in all solvent systems, **4** was essentially inactive towards HDO of the substrate in any of the solvent investigated realizing <2% conversion to HDO products under the same reaction conditions as listed in Table 2.

One further step back from 2,5-DMF in the C₆ value chain shown in Scheme 1 is 5-hydroxy-methylfurfural (HMF). However, the aldehyde functional group of this substrate makes it even more reactive towards decomposition than 2,5-DMF and we previously found that only intractable resins are formed when attempting the HDO of HMF or furfural using **1** under aqueous acidic conditions [28]. Therefore we postulated that the HDO of HMF directly by **4** is also unlikely to succeed. Instead the HDO of the longer chain substrate 4-(5-methyl-2-furanyl)-3-buten-2-one (in the following denoted as C9 substrate) obtained by a Zinc proline complex catalyzed aldol condensation of 5-methyl-furfural with acetone was attempted [26,29]. The C9 substrate is a model for the aldol condensation adduct of HMF with acetone, lacking only the furanic methanol group which can be converted to methyl by hydrogenolysis [30,31]. The subsequent formation of an aldol adduct replaces the aldehyde group of HMF with an α,β -unsaturated ketone, greatly reducing the (self)-reactivity and making HDO by **4** potentially possible.

Scheme 6 details the formation and conversion pathways of the C9 substrate that rationalize the results of the HDO this substrate



Scheme 5. Acid catalyzed formation of $[\text{Ru}(4'\text{-Ph-terpy})_2]^{2+}$ from **4**.

by **4** as given in Fig. 1. At a catalyst load of 1.0% w.r.t. substrate, complex **4** is capable of producing 2,5,8-nonatriol (**10**) from this substrate in 29% yield via hydrogenation of the α,β -unsaturated side chain, followed by ring opening and hydrogenation of all carbonyl groups along with a combined 34% yield of the other partially hydrogenated intermediates identified by mass spectrometry (M^+ peaks and fragmentation patterns under CI conditions) and listed in Fig. 1.

3.3. DFT calculations

The reaction conditions and requirement to use high-pressure reactors make mechanistic studies and observation of any reactive intermediates derived from **4**, notably any postulated hydride complex, very challenging.⁴ We therefore probed conceivable reaction pathways for hydrogen activation and hydride transfer by DFT calculations. One of the reasons for selection of the quS ligand was the desire to incorporate the potential for a metal–ligand bifunctional (MLB) hydrogenation mechanism. To allow an MLB mechanism, the sulfur atom of the quS ligand must be *cis* to coordinated H_2 during the catalytic cycle. However, based on the geometry of **4** established by NMR (NOE experiment), the sulfur atom of quS is not aligned in the desired manner in the pro-catalyst, but is in fact *trans* to the labile acetonitrile ligand to be displaced by H_2 . Nonetheless, an MLB mechanism may be possible if reorganization of the quS ligand in the coordination sphere via a 5-coordinate transition state is energetically feasible. Therefore in order to predict if an MLB mechanism could be operating, the energy profiles for a concerted MLB, stepwise MLB and non-MLB hydrogenation mechanism were investigated *in silico* for the hydrogenation of formaldehyde as a model carbonyl substrate. The calculated energy profiles are shown in Fig. 2.

Formaldehyde was chosen due to the difficulties in locating transition states with the larger carbonyl substrates studied experimentally. Although formaldehyde has lower steric bulk than 2,5-hexanedione, steric effects should contribute relatively equally in the hydride transfer steps of all proposed reaction pathways, and therefore calculations with formaldehyde as a model carbonyl substrate were deemed to be useful for mechanistic insight.

The reaction pathway following a concerted MLB mechanism possessed the lowest activation barriers, with no individual barrier exceeding 22 kcal/mol. Although the initial activation barrier for H_2 coordination *trans* to the sulfur atom of quS was slightly lower than the barrier for rearrangement of the quS ligand in the coordination sphere, the subsequent barrier to the activation of the coordinated H_2 in this non-MLB pathway was very high, therefore favoring de-coordination of H_2 rather than deprotonation (i.e., rather than heterolytic activation of the coordinated H_2). In con-

trast, once the quS ligand rearranged, all the activation barriers along the proposed concerted MLB pathway were lower than the energies of even the ruthenium hydride *intermediates* formed in the non-MLB or stepwise MLB mechanisms. Transition states for hydride transfer from either geometry of the neutral ruthenium-hydride intermediate formed by deprotonation of the coordinated thiol to protonated or neutral formaldehyde could not be located as reflected by the termination of the reaction pathways from these species in Fig. 2. A geometry for the deprotonation of the *trans* η^1 -dihydrogen complex at $E = 49.54$ kcal/mol, e.g., by H_2O , could not be determined. Instead the acidic distal proton shows a weak interaction with the C–H bond adjacent to the nitrogen atom in the quS ligand.⁵

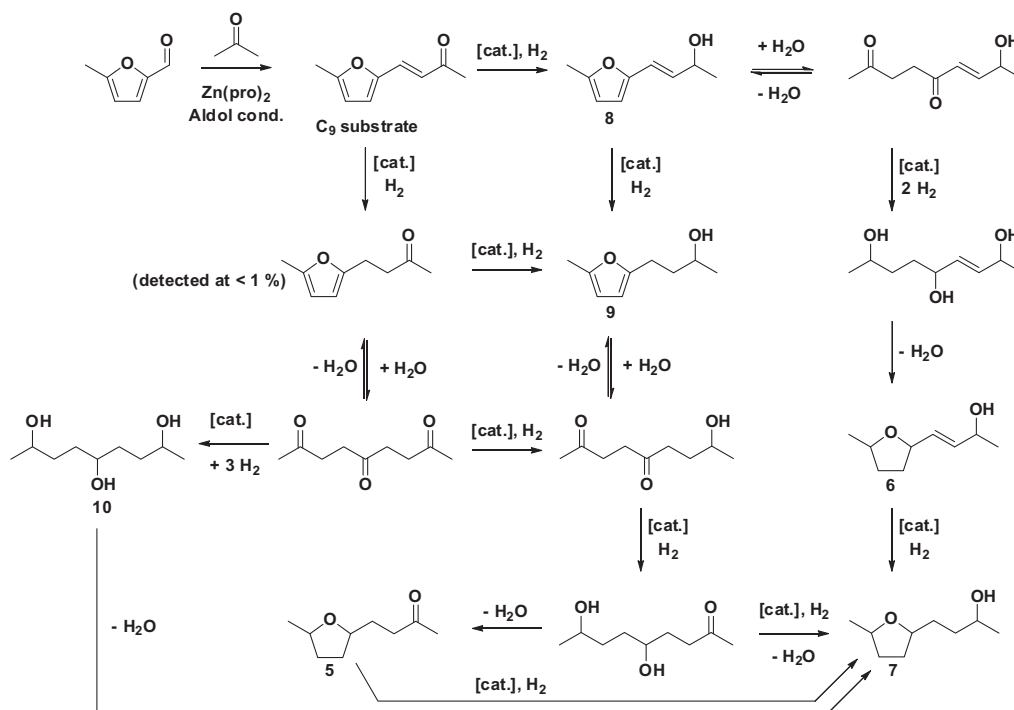
4. Discussion

The addition of a bipy ligand to the coordination sphere of **1** proved detrimental to catalyst activity. The minimum TOF decreased from 125 h^{-1} to only 14 h^{-1} at $200\text{ }^\circ\text{C}$. A possible explanation for this diminished activity are steric constraints imposed by the ligand framework, which would likely have been of limited relevance for the small C1 species used by Creutz et al. [7], but could result in a slower and less active catalyst for the sterically more demanding C6 substrates tested here. Further, the presence of only one free coordination site, while theoretically effective for preventing coordinative inhibition by chelating ligands, would increase the susceptibility to coordinative inhibition by solvent, counterion and other monodentate ligands, potentially explaining the observation that in an actual catalytic cycle the activity of **3** is less than 1/3 that of **1**. Since the binding energy of aqua ligands is expected to be similar to that of coordinated dihydrogen [32–34], and a large excess of available aqua ligands exists in aqueous medium, competition between water and H_2 for the one available coordination site could be another factor explaining the observed TOF for **3** of only 11% of that observed for **1**. It is also conceivable that changes in the electronic environment at the Ru centre caused by the addition of the bipy ligand resulted in a higher activation barrier for the activation of H_2 or hydride transfer to substrate (as the anticipated rate determining steps) compared to **1**, resulting in a slower catalyst turnover.

The relative product distribution between 2,5-DMTHF and 2,5-HDO exhibited a very similar temperature dependence to the product distribution of reactions catalyzed by **1**. This suggests the same reaction cascade and supports the hypothesis that **1** and **3** operate via similar mechanisms of H_2 coordination, deprotonation forming a Ru–H species and then hydride transfer to (protonated) substrate. As elaborated for catalytic hydrogenations with **1** [1], the actual hydrogenation substrate in all reactions

⁴ A direct observation of hydride complexes might be possible through the use of high-pressure NMR, which however is at present beyond our capabilities.

⁵ See Supplementary Material for detailed energies and Cartesian coordinates for all species shown in Fig. 2.



Scheme 6. Reaction cascade for the HDO of 4-(5-methyl-2-furanyl)-3-buten-2-one (**C9**) by **4**.

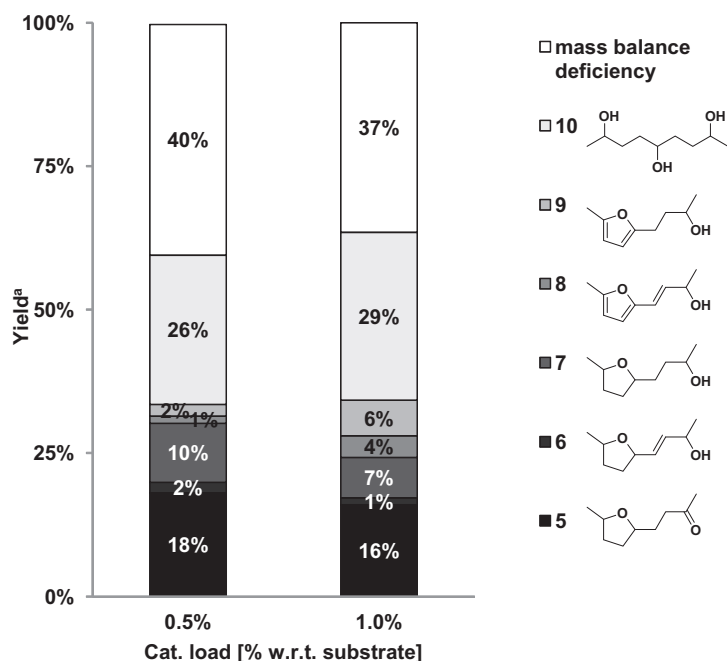


Fig. 1. Results of HDO of the C9 substrate in water.

^aReaction conditions: 4-(5-methyl-2-furanyl)-3-buten-2-one [500 mmol/L] in water, 55 bar (800 psi) H₂(g), dimethylsulfone (ISTD) [100 mmol/L], reaction temperature = 200 °C, reaction time = 16 h. By quant. GC-FID; ±1%; mass balance deficiency = gas phase products and substrate decomposition to polymers and solids (humins) not quantifiable by GC; product identification by GC-MS.¹⁹

is 2,5-HD, i.e., starting from 2,5-DMF, the first step is hydrolysis of the furan ring to the 2,5-HD, while a direct hydrogenation of the furan ring to 2,5-DMTHF does not occur.

The addition of the quS ligand to the coordination sphere of **1** to form **4** did not have a detrimental effect on the reaction rate with the minimum TOF achieved with **4** being comparable to that of **1** at 121 h⁻¹ compared to 125 h⁻¹. Since **4**, like **3**, has only one potential free coordination site available for H₂ binding and activation, this

therefore suggests that a different mechanism is operating with this catalyst allowing faster turn over at the single active site in spite of a similar steric environment and greater selectivity for diol formation without condensation to oxacyclic THF rings.

Based on the result of the DFT study that suggested that an initial dissociation of acetonitrile followed by isomerization of the 5-coordinate intermediate to a *cis* geometry (as proposed in Scheme 2) is possible and actually leads to reaction pathway with

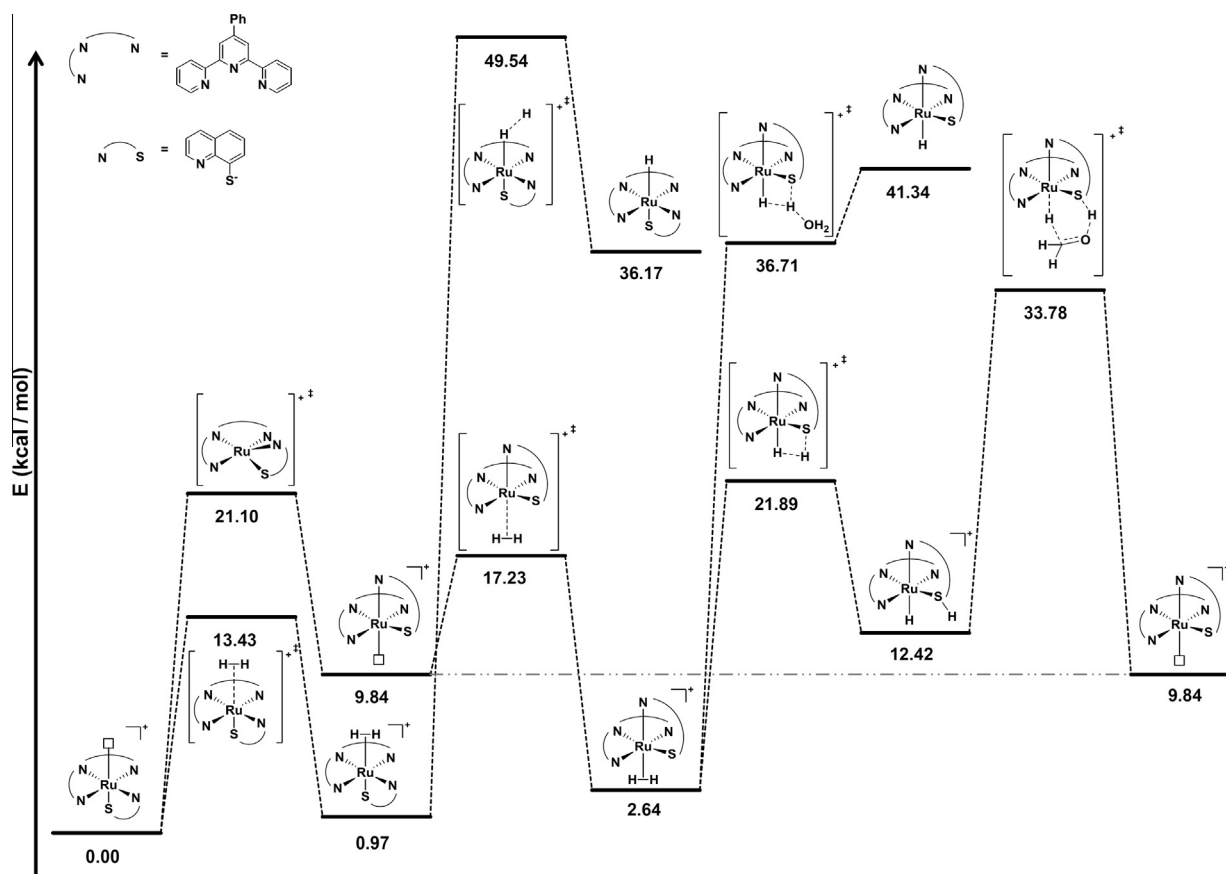


Fig. 2. Energy profiles (kcal/mol) for the hydrogenation of formaldehyde by **4** via concerted MLB, stepwise MLB and non-MLB mechanisms.^a

^aM06-L/[6-311G(d,p) (C,H,N,S,O) def2-TZVP (Ru)]//M06-L/[6-31G(d,p) (C,H,N,S,O) def2-SVP (Ru)] level of theory with polarizable continuum model for water.

lower activation barriers, the three most likely mechanisms for hydrogenation catalyzed by **4** are shown in Scheme 7. The higher energy non-MLB pathway shown (top half of Scheme 7) would be analogous to that presumably followed by **1** and **3**. The two potential MLB pathways however (bottom half of Scheme 7), either concerted or stepwise, are mechanisms not accessible by **1** or **3**. We therefore propose this to be at least part of the explanation for the much higher activity of **4** compared to **3** with the other factor being a different, more electron-rich electronic environment imparted on the ruthenium centre by the soft sulfur donor atom, which in turn could substantially enhance the hydride donor ability of the postulated hydride complex. To our knowledge this is only the second example of a possible metal–ligand bifunctional hydrogenation under aqueous acidic conditions, the other being the comparison between the complexes $[(\eta^5\text{-C}_5\text{H}_5)\text{Ru}(2,2'\text{-bipyridine})(\text{L})\text{OTf}]$ versus $[(\eta^5\text{-C}_5\text{H}_5)\text{Ru}(6,6'\text{-diamino-2,2'\text{-bipyridine})(\text{L})\text{OTf}]$; (L = labile ligand) reported by us earlier [35].

The strong preference for proton and hydride transfer within the coordination sphere of the complex rather than deprotonation of $\eta^2\text{-H}_2$ complexes of **4** by solvent/substrate may also explain the much higher selectivity for 2,5-HDO formation by **4** compared to **1** or **3**. Since 2,5-DMTHF is formed by acid catalyzed ring closure of 2,5-HDO [1,29], and reactions catalyzed by **4** potentially avoid releasing free acid (as H_3O^+ in the solvent leveled acid in the aqueous medium) this may explain the much higher selectivity for production of 2,5-HDO by this catalyst.

The production of significant amounts of 2,5,8-nonanetriol by the HDO of 4-(5-methyl-2-furanyl)-3-buten-2-one (C9) by **4** is significant as this product could be extremely valuable as a potential renewable biomass-based polymer cross-linker, e.g., for polyurethanes or polyesters. While such a process facilitated by **4** or other

similar catalysts is at present hampered by the limited availability of the C9 and similar substrates and would also require further optimization, it is already preferable to the production via conventional synthetic routes involving multiple steps and extremely low atom efficiency.⁶ To the authors' knowledge only one reported synthesis of 2,5,8-nonanetriol exists in the literature [36], which requires seven steps.⁷ While the overall yield is 52% the synthesis involves two Grignard reactions, one oxidation using the Dess–Martin periodinane and protection and deprotection using silanes, all of which generate stoichiometric waste products, in addition to requiring several different organic solvents and quenching reagents resulting in a very unfavorable e-factor [37]. In comparison, the production of 2,5,8-nonanetriol in the current work generates no stoichiometric waste products, is performed in water and all starting materials are – in principle – available from a renewable biomass substrates.⁸

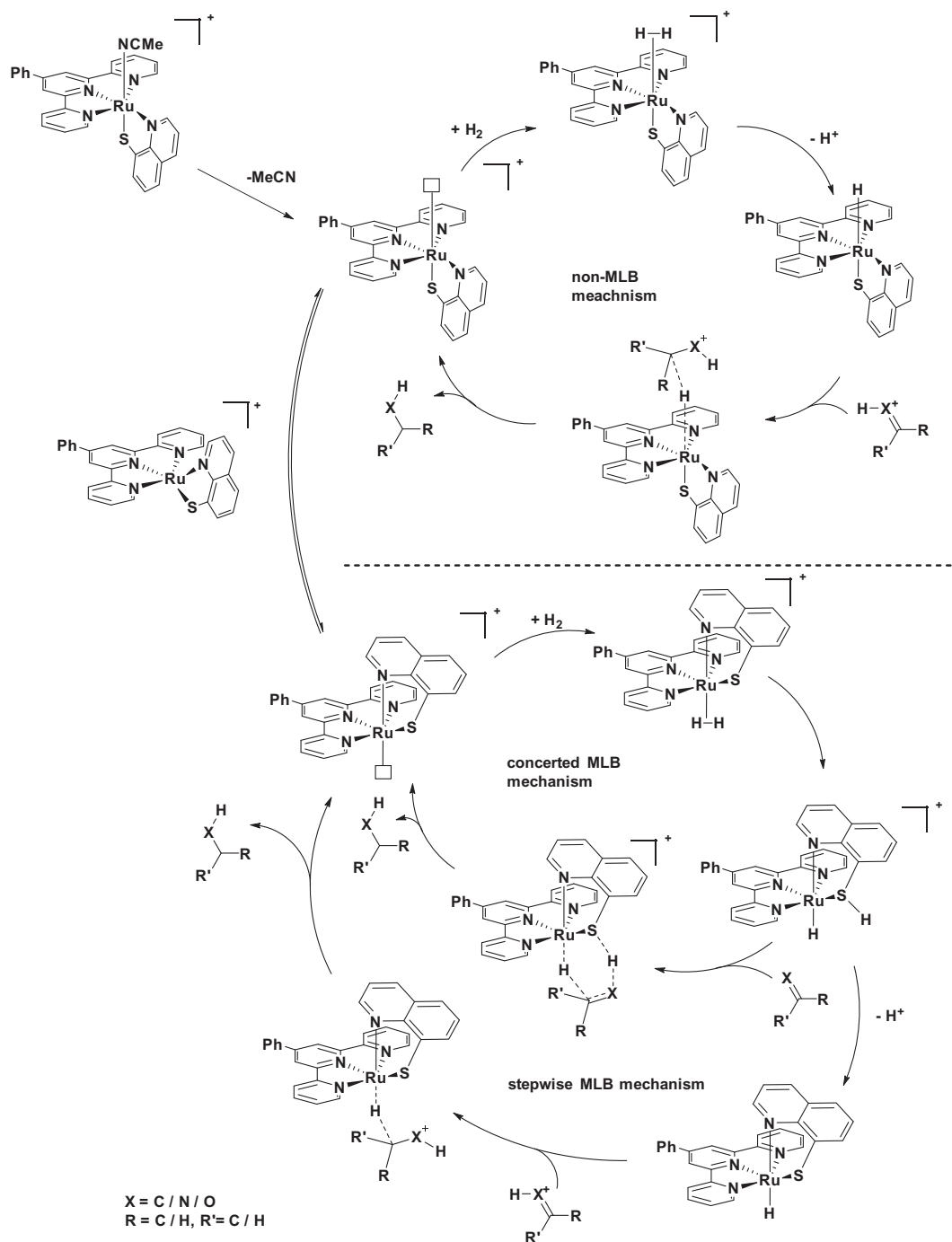
5. Conclusions

The addition of the quS ligand to the coordination sphere of **1**, generating **4**, increased the TON by slowing the formation of the bis-chelate **2**, however complete prevention of this deactivation pathway was not realized. In water at 200 °C, **4** proved effective for the production of 2,5-hexanediol from either 2,5-hexanedione

⁶ At present no commercial source for the acetone aldol adducts with HMF or furfural exists.

⁷ The complete synthetic sequence is shown in the Supplementary Material (Scheme SM1).

⁸ Note that acetone is available by fermentation of sugars/starch via the ABE process or through the ketonization of acetic acid.



Scheme 7. Proposed concerted MLB, stepwise MLB and non-MLB mechanisms for the heterolytic activation of dihydrogen and hydrogenation of carbonyls by **4**.

or 2,5-dimethylfuran in good yield (up to 82% and 78% respectively) and with much higher selectivity than achieved by **1**. Furthermore, 2,5,8-nonanetriol could be produced from the C9 substrate (a model for the aldol condensation adduct of HMF with acetone) in 29% yield demonstrating that high value added chemicals difficult to manufacture from typical fossil fuel feedstocks can be easily produced from biomass substrates using homogeneous catalysis.

Comparison of the catalytic activity between **4** and **3** suggests that **4** operates by an MLB mechanism, which is supported by an *in silico* investigation of the reaction mechanism for hydrogenation of formaldehyde as a model carbonyl substrate by **4**. This study also provided a possible explanation for the observed high

2,5-hexanediol selectivity, since the predicted mechanism involved concerted proton and hydride transfer between the metal complex and the substrate and therefore did not generate free acid (H_3O^+) that would catalyze the ring closure of 2,5-hexanediol to 2,5-DMTHF.

Acknowledgements

The authors thank the Natural Science and Engineering Council (NSERC) Canada, the Bioeconomy Program of the Ontario Ministry for Agriculture, Food and Rural Affairs (OMAFRA) and the Los Alamos National Laboratory (LANL) Laboratory Directed Research and Development (LDRD) program for supporting this research.

Appendix A. Supplementary data

Compound Data Sheets with images of NMR/MS/IR spectra of all relevant ligands and complexes. Example Micro-GC, GC and GC–MS data. Detailed results (energies and Cartesian coordinates) of Gaussian calculations (75 pages). Supplementary data associated with this article can be found, in the online version, at <http://dx.doi.org/10.1016/j.poly.2015.10.049>.

References

- [1] R.J. Sullivan, E. Latifi, B.K.M. Chung, D.V. Soldatov, M. Schlaf, *ACS Catal.* (2014) 4116.
- [2] B. Saha, M.M. Abu-Omar, *ChemSusChem* 8 (2015) 1133.
- [3] D. Taher, M.E. Thibault, D.D. Mondo, M. Jennings, M. Schlaf, *Chem. Eur. J.* (2009) 10132.
- [4] M. Schlaf, *J. Chem. Soc., Dalton Trans.* (2006) 4645.
- [5] Y. Matsubara, E. Fujita, M.D. Doherty, J.T. Muckerman, C. Creutz, *JACS* 134 (2012) 15743.
- [6] C. Creutz, M.H. Chou, H. Hou, J.T. Muckerman, *Inorg. Chem.* 49 (2010) 9809.
- [7] C. Creutz, M.H. Chou, *J. Am. Chem. Soc.* 129 (2007) 10108.
- [8] M. Schlaf, R.H. Morris, *J. Chem. Soc., Chem. Commun.* (1995) 625.
- [9] M. Schlaf, A.J. Lough, R.H. Morris, *Organometallics* 15 (1996) 4423.
- [10] S.C. Rasmussen, S.E. Ronco, D.A. Mlsna, M.A. Billadeau, W.T. Pennington, J.W. Kolis, J.D. Petersen, *Inorg. Chem.* 34 (1995) 821.
- [11] M.J. Frisch, G.W. Trucks, H.B. Schlegel, G.E. Scuseria, M.A. Robb, J.R. Cheeseman, G. Scalmani, V. Barone, B. Mennucci, G.A. Petersson, H. Nakatsuji, M. Caricato, X. Li, H.P. Hratchian, A.F. Izmaylov, J. Bloino, G. Zheng, J.L. Sonnenberg, M. Hada, M. Ehara, K. Toyota, R. Fukuda, J. Hasegawa, M. Ishida, T. Nakajima, Y. Honda, O. Kitao, H. Nakai, T. Vreven, J.A. Montgomery Jr., J.E. Peralta, F. Ogliaro, M.J. Bearpark, J. Heyd, E.N. Brothers, K.N. Kudin, V.N. Staroverov, R. Kobayashi, J. Normand, K. Raghavachari, A.P. Rendell, J.C. Burant, S.S. Iyengar, J. Tomasi, M. Cossi, N. Rega, N.J. Millam, M. Klene, J.E. Knox, J.B. Cross, V. Bakken, C. Adamo, J. Jaramillo, R. Gomperts, R.E. Stratmann, O. Yazyev, A.J. Austin, R. Cammi, C. Pomelli, J.W. Ochterski, R.L. Martin, K. Morokuma, V.G. Zakrzewski, G.A. Voth, P. Salvador, J.J. Dannenberg, S. Dapprich, A.D. Daniels, Ö. Farkas, J.B. Foresman, J.V. Ortiz, J. Cioslowski, D.J. Fox, in: *Gaussian, Inc., Wallingford, CT, USA*, 2009.
- [12] Y. Zhao, D.G. Truhlar, *J. Chem. Phys.* 125 (2006) 194101.
- [13] Y. Zhao, D.G. Truhlar, *Theor. Chem. Acc.* 120 (2008) 215.
- [14] F. Weigend, R. Ahlrichs, *Phys. Chem. Chem. Phys.* 7 (2005) 3297.
- [15] D. Andrae, U. Haussermann, M. Dolg, H. Stoll, H. Preuss, *Theoret. Chim. Acta* 77 (1990) 123.
- [16] W.J. Hehre, R. Ditchfie, J.A. Pople, *J. Chem. Phys.* 56 (1972) 2257.
- [17] P.C. Hariharan, J.A. Pople, *Theoret. Chim. Acta* 28 (1973) 213.
- [18] M.M. Francl, W.J. Pietro, W.J. Hehre, J.S. Binkley, M.S. Gordon, D.J. Defrees, J.A. Pople, *J. Chem. Phys.* 77 (1982) 3654.
- [19] S. Miertus, E. Scrocco, J. Tomasi, *Chem. Phys.* 55 (1981) 117.
- [20] S. Miertus, J. Tomasi, *Chem. Phys.* 65 (1982) 239.
- [21] J.L. Pascualahir, E. Silla, I. Tunon, *J. Comput. Chem.* 15 (1994) 1127.
- [22] V. Barone, M. Cossi, J. Tomasi, *J. Comput. Chem.* 19 (1998) 404.
- [23] M. Cossi, G. Scalmani, N. Rega, V. Barone, *J. Chem. Phys.* 117 (2002) 43.
- [24] R. Krishnan, J.S. Binkley, R. Seeger, J.A. Pople, *J. Chem. Phys.* 72 (1980) 650.
- [25] A.D. McLean, G.S. Chandler, *J. Chem. Phys.* 72 (1980) 5639.
- [26] L.A. Silks, J.C. Gordon, R. Wu, S.K. Hanson, in: *Los Alamos National Security, LLC, USA*, 2011, WO2011022042A1. Chemical Indexing Equivalent to 154:234477 (US).
- [27] K. Alder, C.H. Schmidt, *Ber. Dtsch. Chem. Ges.* 76 (1943) 183.
- [28] Oswin, C.T., (M.Sc. Thesis), University of Guelph, 2013.
- [29] A.D. Sutton, F.D. Waldie, R. Wu, M. Schlaf, L.A. 'Pete' Silks, J.C. Gordon, *Nat. Chem.* 5 (2013) 428.
- [30] Y.B. Huang, M.Y. Chen, L. Yan, Q.X. Guo, Y. Fu, *ChemSusChem* 7 (2014) 1068.
- [31] M.R. Grochowski, W.R. Yang, A. Sen, *Chem. – Eur. J.* 18 (2012) 12363.
- [32] G.J. Kubas, *J. Organomet. Chem.* 635 (2001) 37.
- [33] P.V. Grundler, O.V. Yazyev, N. Aebischer, L. Helm, G. Laurenczy, A.E. Merbach, *Inorg. Chim. Acta* 359 (2006) 1795.
- [34] G. Kubas, *Metal Dihydrogen and σ -Bond Complexes. Structure, Theory and Reactivity*, Kluwer Academic/Plenum Publishers, New York, 2001.
- [35] D. DiMondo, M.E. Thibault, J. Britten, M. Schlaf, *Organometallics* 32 (2013) 6541–6554.
- [36] K.K. Thota, M.L. Trudell, *Synthesis-Stuttgart* 45 (2013) 2280–2286.
- [37] R.A. Sheldon, *Green Chem.* 9 (2007) 1273–1283.